Dalton Transactions

PAPER

View Article Online
View Journal | View Issue

Cite this: *Dalton Trans.*, 2016, **45**, 6023

Exploring structural and electronic effects in three isomers of tris{bis(trifluoromethyl)phenyl}borane: towards the combined electrochemical-frustrated Lewis pair activation of H_2†

Robin J. Blagg,*[a] Elliot J. Lawrence,*[a] Katie Resner,[a] Vasily S. Oganesyan,[a] Thomas J. Herrington,[b] Andrew E. Ashley[b] and Gregory G. Wildgoose*[a]

Received 21st May 2015,
Accepted 22nd July 2015

DOI: 10.1039/c5dt01918d

www.rsc.org/dalton

Three structural isomers of tris{bis(trifluoromethyl)phenyl}borane have been studied as the acidic component of frustrated Lewis pairs. While the 3,5-substituted isomer is already known to heterolytically cleave H_2 to generate a bridging-hydride; *ortho*-substituents in the 2,4- and 2,5-isomers quench such reactivity through electron donation into the vacant boron p_z orbital and steric blocking of the boron centre; as shown by electrochemical, structural and computational studies. Electrochemical studies of the corresponding borohydrides identify that the two-electron oxidation of terminal-hydrides occurs at more positive potentials than observed for $[HB(C_6F_5)_3]^-$, while the bridging-hydride oxidizes at a higher potential still, comparable to that of free H_2.

Introduction

Since the pioneering work of Stephan's group[1] the field of frustrated Lewis pair (FLP) chemistry has grown rapidly.[2–7] The archetypal FLP system combines the Lewis acid $B(C_6F_5)_3$ with a sterically demanding Lewis base such as $P(^tBu)_3$, to effect the heterolytic cleavage of H_2, resulting in the formation of the corresponding hydridic and protic products respectively.

FLPs have found applications as catalysts or mediators for a variety of reactions such as the metal-free hydrogenation of imines and nitriles,[8] alkynes,[9] silyl enol ethers,[10] and ketones.[11,12] The activation of small molecules such as CO_2,[13,14] and alkynes by FLPs has also found applications in the synthesis of heterocycles and other aromatic systems.[15]

While much of the literature has focused on tris(pentafluorophenyl)borane, $B(C_6F_5)_3$ as the Lewis acidic component in FLPs, other electron-deficient boranes have been used, including a range of halogenated triarylboranes,[14,16–18] and borenium cations,[19,20] Other examples of Lewis acids that have found use in FLPs include: the triaryl aluminium species, $Al(C_6F_5)_3$, which generates a bridging-hydride following cleavage of H_2;[21] and the carbon based *N*-methylacridinium salts which activate H_2 even in the presence of H_2O.[22] FLPs are not limited to the main group, with zirconocene–phosphane complexes pioneered by Wass and co-workers shown to act as intramolecular FLPs that exhibit unprecedented reactivity towards small molecules;[23] similar chemistry has also been demonstrated with zirconocene-amines which act as hydrogenation catalysts with a wide range of substrates.[24]

In 2014 we introduced the concept of "combined electrochemical-frustrated Lewis pairs",[20,25,26] that couple the heterolytic cleavage of H_2 by a conventional FLP with *in situ* electrochemical oxidation of the resultant borohydride and subsequent regeneration of the parent borane. The combined electrochemical-FLP systems were shown to be electrocatalytic for the oxidation of H_2 (to form two protons and two electrons – a key reaction in many hydrogen-based energy technologies). These preliminary reports represent the first application of FLP chemistry other than to catalyse the hydrogenation of small molecules. For example, by combining the archetypal $B(C_6F_5)_3/P(^tBu)_3$ FLP in the presence of H_2 whilst at the same time oxidizing the resultant $[HB(C_6F_5)_3]^-$ intermediate formed, the potential for oxidation (the energetic driving force) of the borohydride at a glassy carbon electrode was found to be reduced by 0.61 V, in comparison to the direct oxidation of H_2 (observed at *ca.* +1.49 V *vs.* $[FeCp_2]^{0/+}$ under the same conditions), an energy saving equivalent to 117.7 kJ mol^{-1}.[25]

Herein we report studies on three isomers of tris{bis(trifluoromethyl)phenyl}borane (Fig. 1) and their associated

[a]*School of Chemistry, University of East Anglia, Norwich, NR4 7TJ, UK. E-mail: r.blagg@uea.ac.uk, elliot.lawrence@uea.ac.uk, g.wildgoose@uea.ac.uk*
[b]*Department of Chemistry, Imperial College London, South Kensington, London, SW7 2AZ, UK*

†Electronic supplementary information (ESI) available: Comprising: annotated ORTEP plot of the X-ray crystal structure of **3**; cyclic voltammograms of $B(C_6F_5)_3$ under corresponding conditions; further computational data. CCDC 1061234. For ESI and crystallographic data in CIF or other electronic format see DOI: 10.1039/c5dt01918d

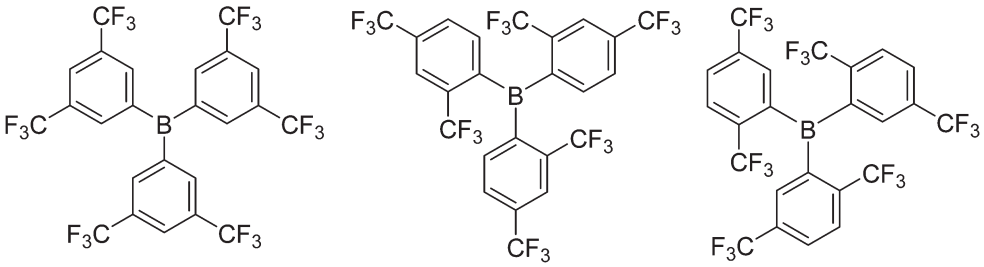

Fig. 1 Isomers of tris{bis(trifluoromethyl)phenyl}borane.

tris{bis(trifluoromethyl)phenyl}borohydrides. Electrochemical and computational investigations explain their varying ability to heterolytically cleave H_2 as part of a FLP and allow us to extend our studies into combined electrochemical-FLPs.

Results and discussion

Synthesis and characterization

The synthesis of tris{3,5-bis(trifluoromethyl)phenyl}borane **1** has been previously reported,[18,27] and whilst a synthetic route to tris{2,4-bis(trifluoromethyl)phenyl}borane **2** has been reported by Cornet *et al.*[28] their method led to a mixture of products requiring the isolation of **2** in low yield by fractional sublimations. The commercial availability of 2,4-bis(trifluoromethyl)bromobenzene and 2,5-bis(trifluoromethyl)bromobenzene allows us to report an improved synthetic route to **2** and also the synthesis of the novel tris{2,5-bis(trifluoromethyl)-phenyl}borane **3**.

Boranes **2** and **3** were synthesized by lithium–halogen exchange of $BrC_6H_3(CF_3)_2$ with ^{n}BuLi at −77 °C generating the aryllithium species $LiC_6H_3(CF_3)_2$. Treatment of this with a third of an equivalent of BCl_3, followed by warming to room temperature, subsequent removal of the volatiles and purification by sublimation or recrystallization allowed for the isolation of pure **2** and **3**, in 90 and 77% yields respectively. It should be noted that applying the same synthetic route for the synthesis of **1**, leads to a mixture of products with $[Li(OEt_2)_n]$-$[B\{3,5\text{-}(CF_3)_2C_6H_3\}_4]$ as the major component.

The crystal structures of **1**[29] and **2**[28] have been previously reported. Single crystals of **3** were obtained by slow diffusion of a saturated CH_2Cl_2 solution of **3** into *n*-hexane at −25 °C, from which the crystal structure was obtained in collaboration with the EPSRC UK National Crystallography Service[30] (Fig. 2 and S1,† and Table 2).

The structures of **1–3** all show similar features, with a trigonal-planar boron centre and the three aryl rings twisted with respect to the BC_3 plane to minimize steric interactions between the aryl rings. The degree of twist can be quantified by an appropriate choice of C–B–C–C torsion angles, which are both smaller and more consistent for **1** {mean 36(2)°, range 33.2–38.9°} than for **2** {mean 54(11)°, range 42.3–68.3°} or **3** {mean 53(9)°, range 40.9–61.2°}, due to the steric bulk of *ortho*-trifluoromethyl substituents. For **2** and **3** this results in the *ortho*-CF_3 groups orientated above/below the boron centre resulting in B···F distances of 2.81(1), 2.80(7) Å for **2** and **3** respectively. The orientation of these groups suggests the possibility of electron donation from the fluorine atoms into the formally vacant p_z orbital at boron; an effect together with the steric influence of the *ortho*-CF_3 groups which would be expected to have a significant influence on the Lewis acidity/reactivity of these compounds. An example of the type of reactivity which could be expected from the *ortho*-CF_3 groups, was observed by Cornet *et al.*, who reported evidence of B–Cl/B–F exchange in mixtures containing the boranes $B(Ar^F)_2Cl$ where Ar^F = 2,4,6-$(CF_3)_3C_6H_2$, 2,4-$(CF_3)_2C_6H_3$ or 2,6-$(CF_3)_2C_6H_3$.[28]

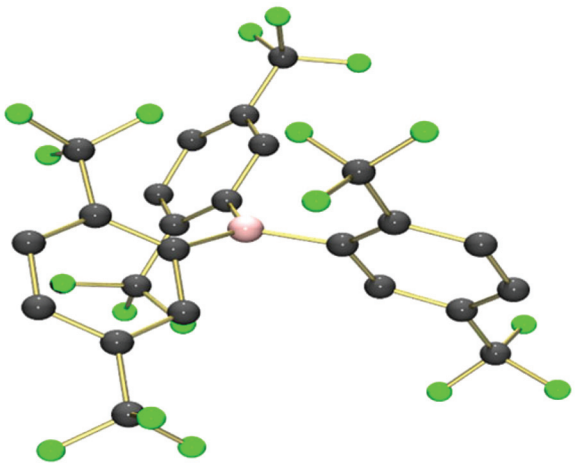

Fig. 2 The crystallographic molecular structure of $B\{2,5\text{-}(CF_3)_2C_6H_3\}_3$ **3** (hydrogen atoms removed for clarity).

The reactivity of **1** as the Lewis acidic component of an FLP has been previously studied,[18] which showed that the reaction of **1** with H_2 in the presence of 2,2,6,6-tetramethylpiperidine (tmp) leads to rapid formation of the bridging hydride species $[tmpH][(\mu\text{-}H)(\mathbf{1})_2]$. Analogous reactions of **2** and **3** with H_2 in the presence of the Lewis bases tmp or $P(^tBu)_3$, result in neither Lewis acid–base adduct formation nor any evidence of

H_2 activation observable by NMR spectroscopy over a minimum period of 48 hours.

Direct synthesis of authentic terminal-hydride species $[HB\{C_6H_3(CF_3)_2\}_3]^-$ proved to be possible for all three isomers **1–3** by direct reaction of the borane with sodium triethylborohydride in toluene solution, resulting in near quantitative conversion to the corresponding borohydrides. NMR spectra of the terminal-hydride species Na[**1**-H]–Na[**3**-H] show doublets in the ^{11}B spectra (δ_B: −9.1, −15.3, −14.2 and $^1J_{BH}$: 88, 93, 84 Hz respectively) and broad 1 : 1 : 1 : 1 quartets in the proton spectra (δ_H: +3.66, +4.06, +3.06 respectively). Additionally, for Na[**2**-H] and Na[**3**-H] clear evidence of through-space coupling between the hydride and *ortho*-CF_3 groups is observed in the ^{19}F spectra (J_{FH} = 6.8, 7.6 Hz respectively); further, in the case of Na[**3**-H] this coupling is also observable in the proton spectrum with the hydride signal observable as a 1 : 1 : 1 : 1 quartet of broad 1 : 3 : 3 : 1 quartets (Fig. 3).

Synthesis of Na[**2**-H] and Na[**3**-H] allows for the confirmation that the inability of the **2**,**3**/P(^{t}Bu)$_3$ FLPs to cleave H_2 is not due to unfavourable thermodynamics, but due to the significant kinetic barrier resulting from the steric and electronic effects of the *ortho*-CF_3 groups. Reaction with authentic $[(^t Bu)_3PH]Cl$ results in rapid metathesis (indicated by precipitation of NaCl) and formation of the salts $[(^t Bu)_3PH][$**2**-H] and $[(^t Bu)_3PH][$**3**-H]. NMR spectra of which, show no liberation of H_2, regeneration of free borane/phosphine, or any other evidence of reaction over a 66 hour period.

Electrochemical studies

Cyclic voltammetric studies of **1–3** were performed in the non-coordinating solvent CH_2Cl_2 using $[^n Bu_4N][B(C_6F_5)_4]$ as the added electrolyte at a glassy carbon electrode (GCE). In all three cases a one-electron, reduction process is observed with *quasi*-reversible (moderately fast) electron transfer kinetics. However for **1** (Fig. 4a) the process appears to be *chemically* irreversible (but not *electrochemically* irreversible) at scan rates up to 2.0 V s^{-1} due to fast chemical follow-up kinetics *cf.* the rate of electron transfer, while for both **2** (Fig. 4b) and **3** (Fig. 4c) an associated oxidation wave is observed indicating

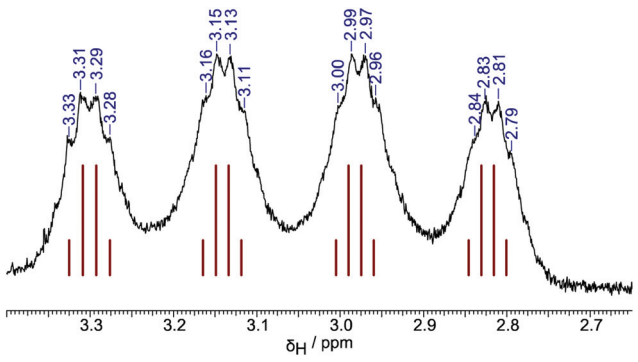

Fig. 3 Hydride resonance in ^1H NMR spectrum of Na[**3**-H], showing coupling to both ^{11}B (I = 3/2) and an *ortho*-CF_3 group {3× ^{19}F, I = 1/2).

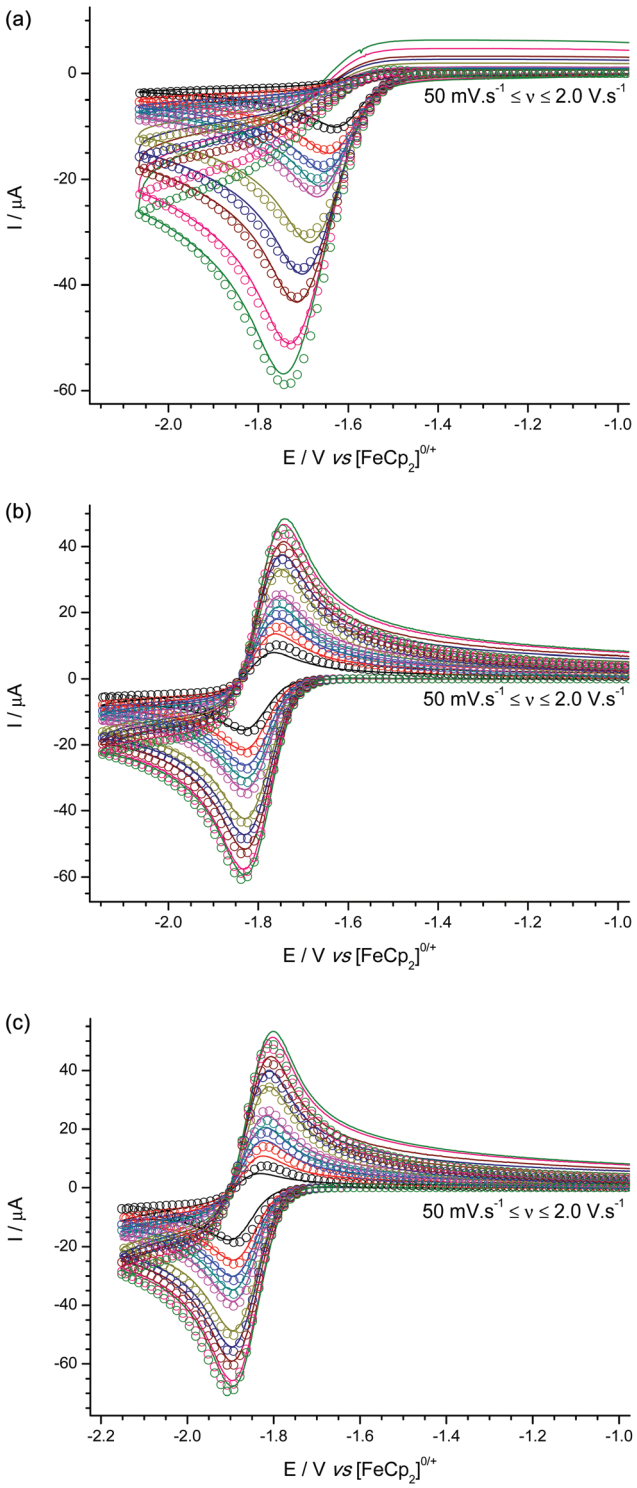

Fig. 4 Experimental (line) and simulated (open circles) cyclic voltammograms for the reduction of (a) **1**, (b) **2**, and (c) **3**.

that the radical anions $\mathbf{2}^{\bullet-}$ and $\mathbf{3}^{\bullet-}$ are sufficiently stable on the electrochemical timescale for their subsequent (re-)oxidation to be observable.

Based on our previous experience from an electrochemical study of $B(C_6F_5)_3$,[31] we performed digital simulations of the

Table 1 Mechanistic parameters obtained by digital simulation of voltammetric data for the one-electron reductions of **1–3**

		1	**2**	**3**
$BArF_{18} + e^- = BArF_{18}^{\bullet -}$	E° *vs.* $[FeCp_2]^{0/+}$/V	−1.61 ± 0.01	−1.79 ± 0.01	−1.85 ± 0.01
	α	0.419	0.498	0.468
	k°/cm s^{-1}	4.56×10^{-3}	2.61×10^{-2}	2.22×10^{-2}
$BArF_{18}^{\bullet -} \Rightarrow$ 'decomposition'	k_f/s^{-1} [b]	≥25	1.92×10^{-2}	8.08×10^{-2}
$D(BArF_{18}) = D(BArF_{18}^{\bullet -})/cm^2\ s^{-1}$ [a]	3.76×10^{-5}	1.13×10^{-5}	1.13×10^{-5}	

[a] Diffusion constants (D) obtained *via* ^1H and ^{19}F DOSY NMR spectroscopy. [b] k_f values are modelled as a *pseudo* first-order process.

experimental voltammetric data modelled using an EC-mechanism (*i.e.* a reversible, heterogeneous electron transfer step followed by an irreversible, homogeneous chemical step which generates electro-inactive products. Other postulated mechanisms produced a poor fit to the data). These digital simulations allowed us to extract pertinent mechanistic parameters such as the formal redox potentials and charge transfer coefficients (E° and α respectively) and kinetic parameters for the electron transfer (k°) and follow-on chemical step (k_f) as shown in Table 1.

The formal reduction potentials (E°) suggest that **1** is the most electrophilic of the three boranes, while **3** is the least. While the difference in electrophilicity between **2** and **3** is consistent with a simplified view of the inductive electron withdrawing effects of the different *meta*- and *para*-(CF_3) group positions based on Hammett parameters $\{\sigma_{meta}(CF_3) = 0.43$ *vs.* $\sigma_{para}(CF_3) = 0.54\}$[32] the relative electrophilicity of **1** cannot be similarly rationalized. This is in part because simple Hammett parameters for *ortho*-(CF_3) substituents do not satisfactorily account for any additional steric and/or electronic effects. We can rationalize the reduced electrophilicity of **2** and **3** in comparison to **1** by considering the electronic effect of having *ortho*-CF_3 groups present in **2** and **3**. As noted above, the crystal structures of **2** and **3** show the *ortho*-(CF_3) groups are positioned at sufficiently close distances above the central BC_3 plane such that donation from the lone pairs on the fluorine atoms into the vacant boron p_z orbital on boron could occur; such donation of electron density would be expected to reduce the electrophilicity of the boron centre, as is observed experimentally by our electrochemical measurements and indicated in electronic structure DFT calculations (*vide infra*).

Furthermore, the steric shielding of the boron centre by the *ortho*-(CF_3) groups in **2** and **3** is qualitatively evident from the observation of more reversible redox processes in the cyclic voltammetric data. Quantitatively this is shown in the values of the rate constants (k_f) obtained from voltammetric digital simulation for the radical anion decomposition step, which is assumed to proceed in a similar fashion as was previously ascertained for the analogous $[B(C_6F_5)_3]^{\bullet -}$ intermediate *via* reaction between solvent molecules and the boron centre in the reduced radical anion intermediates, $\mathbf{1}^{\bullet -}$, $\mathbf{2}^{\bullet -}$, or $\mathbf{3}^{\bullet -}$.[31] The value of k_f is at least three orders of magnitude greater for the decomposition of $\mathbf{1}^{\bullet -}$ than for $\mathbf{2}^{\bullet -}$ or $\mathbf{3}^{\bullet -}$, where, in the latter two cases, the presence of *ortho*-CF_3 groups provides significant steric shielding to the boron centre. It is worth noting here that these findings demonstrate the ease with which synthetic chemists working in this area can gain powerful insights into the chemistry of Lewis acidic species by the application of simple, rapid electrochemical characterization techniques in addition to the more ubiquitous crystallographic and spectroscopic characterization techniques. Simple examination of the *shape* and *position* of the voltammetry of each borane, obtained in a 20 minute experiment using inexpensive equipment can tell us qualitatively that in comparison to **1**, boranes **2** and **3** are more sterically hindered, and less electrophilic, and therefore less Lewis acidic and less likely to be active FLP components for H_2 activation. The voltammetry even allows us to infer *why* this is so, given that the only thing boranes **2** and **3** have that **1** does not have and that could simultaneously sterically shield the borane *and* reduce the electronic demand at the boron centre are the *o*-CF_3 groups.

Table 2 Crystallographic data for **3**

	$B\{2,5\text{-}(CF_3)_2C_6H_3\}_3$ **3**
Empirical formula	$C_{24}H_9BF_{18}$
Formula weight	650.12
Temperature/K	100
Crystal system	Triclinic
Space group	$P\bar{1}$
a/Å	7.2951(5)
b/Å	10.6358(7)
c/Å	15.9794(11)
α/°	85.950(4)
β/°	86.582(4)
γ/°	74.846(4)
Volume/Å^3	1192.64(14)
Z	2
ρ_{calc}/mg mm^{-3}	1.810
μ/mm^{-1}	0.204
F(000)	640.0
Crystal size/mm^3	0.30 × 0.06 × 0.02
Radiation	Mo Kα (λ = 0.71075 Å)
2Θ range for data collection	3.974 to 54.96°
Index ranges	$-9 \le h \le 8$, $-13 \le k \le 13$, $-20 \le l \le 20$
Reflections collected	17 457
Independent reflections	5459 [R_{int} = 0.0820, R_{sigma} = 0.0575]
Data/restraints/parameters	5459/0/388
Goodness-of-fit on F^2	1.055
Final R indexes [$I \ge 2\sigma(I)$]	R_1 = 0.0555, wR_2 = 0.1508
Final R indexes [all data]	R_1 = 0.0712, wR_2 = 0.1631
Largest diff. peak/hole/e A^{-3}	0.56/−0.39

In comparison with the archetypal Lewis acid, $B(C_6F_5)_3$ {which is observed under the same conditions as a quasi-reversible reduction at E° = −1.518 V *vs.* $[FeCp_2]^{0/+}$ (see Fig. S2†)}, boranes **1–3** are all less electrophilic; while $[B(C_6F_5)_3]^{\bullet-}$ is more stable (smaller k_f) with respect to follow-on decomposition reactions than $\mathbf{1}^{\bullet-}$, but still considerably less stable than the *ortho*-(CF_3) stabilized $\mathbf{2}^{\bullet-}$ and $\mathbf{3}^{\bullet-}$.

Borohydride oxidation. Our combined electrochemical-FLP concept requires the electrochemical oxidation of borohydrides generated by the heterolytic cleavage of H_2. Despite the only such species generated from the $B\{C_6H_3(CF_3)_2\}_3$ isomers, being the previously reported bridging hydride $[(\mu\text{-H})(\mathbf{1})_2]^-$,[18] the ease of direct synthesis of the terminal hydrides $[HB\{C_6H_3(CF_3)_2\}_3]^-$ allows for their electrochemical study, to add to our understanding of the electrochemistry of the triarylborohydrides. Therefore, electrochemical studies of Na[**1**-H]–Na[**3**-H] and [tmpH][(μ-H)(**1**)$_2$] were performed under the same conditions as their borane precursors (although Na[**1**-H] and [tmpH][(μ-H)(**1**)$_2$] proved only sparingly soluble in CH_2Cl_2, and hence their concentrations cannot be accurately determined). In all cases a single irreversible oxidation wave is observed at scan rates up to 2.0 V s^{-1}.

For the terminal hydrides Na[**1**-H]–Na[**3**-H] (Fig. 5a–c) oxidations occurred with peak potentials of +1.08, +1.31, +1.13 V *vs.* $[FeCp_2]^{0/+}$ at a scan rate of 100 mV s^{-1} respectively; with no evidence of electroactive product species (such as the parent boranes) being regenerated in sufficient quantities to be observed.

The bridging hydride [tmpH][(μ-H)(**1**)$_2$] (Fig. 6) oxidation is observed as a shoulder on the edge of the solvent window, at *ca.* +1.55 V *vs.* $[FeCp_2]^{0/+}$ at a scan rate of 100 mV s^{-1} (observable distinct to the solvent/electrolyte breakdown at scan rates below 1.0 V s^{-1}), trace amounts of the terminal hydride species $[\mathbf{1}\text{-H}]^-$ are also observed. Following oxidation of $[(\mu\text{-H})(\mathbf{1})_2]^-$, sweeping to negative potentials results in observation (at 100 mV s^{-1} scan rate and above) of an irreversible reduction wave at *ca.* −1.7 V *vs.* $[FeCp_2]^{0/+}$ characteristic of the reduction wave observed for the parent borane **1**.

In comparison to our previous studies on $[HB(C_6F_5)_3]^-$,[25] all of the terminal-hydrides oxidize at more positive potentials,

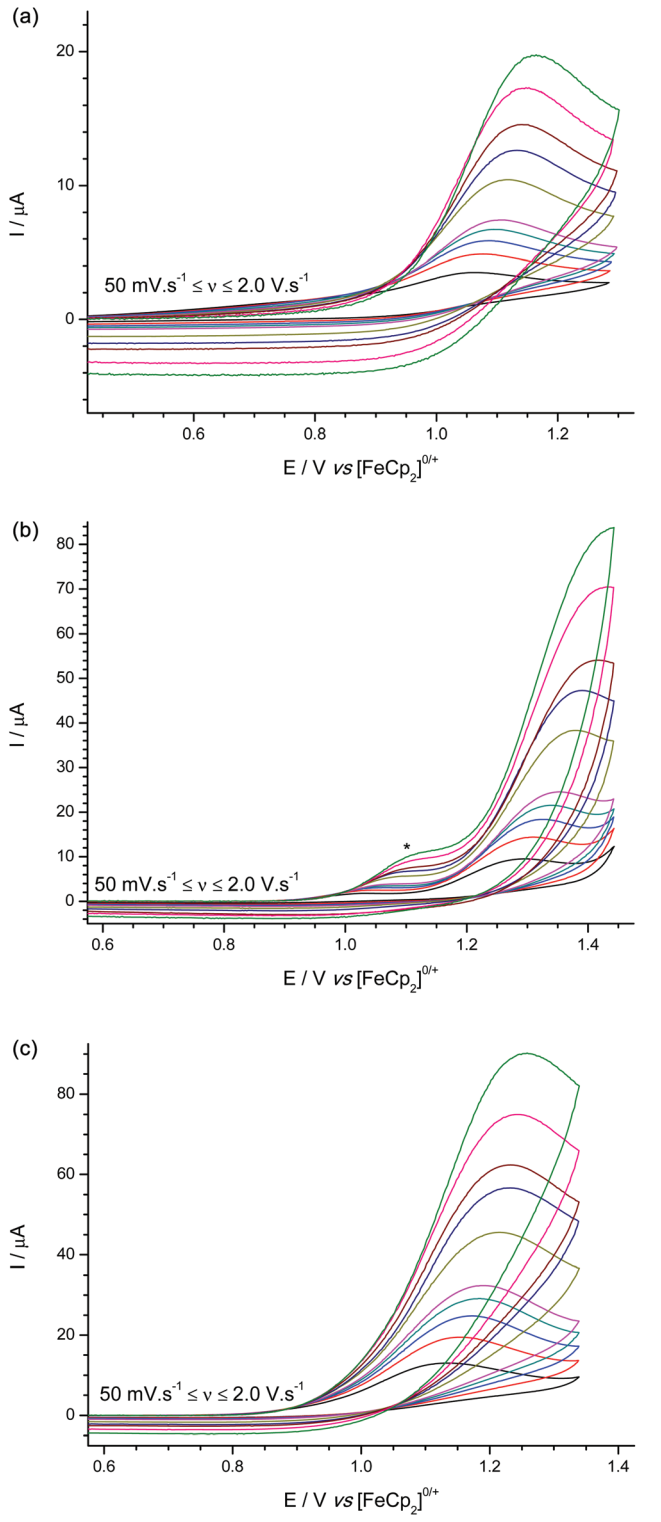

Fig. 5 Experimental cyclic voltammograms for the oxidation of (a) Na[**1**-H], (b) Na[**2**-H], and (c) Na[**3**-H] shoulder (*) visible at the higher scan rates due to trace impurity in the solvent/electrolyte.

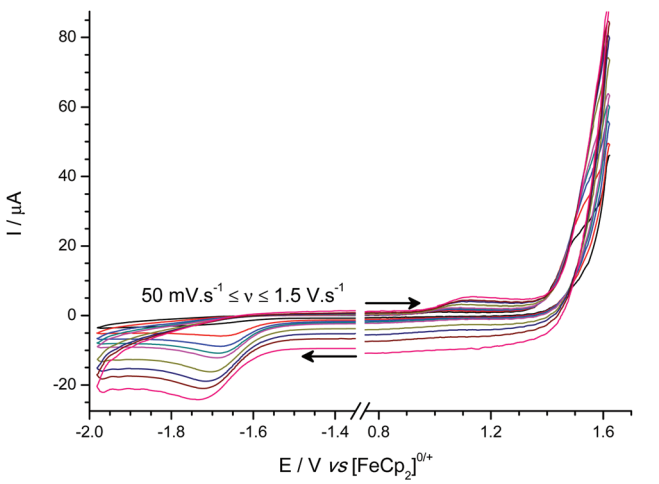

Fig. 6 Experimental cyclic voltammogram(s) for the oxidation of [tmpH][(μ-H)(**1**)$_2$].

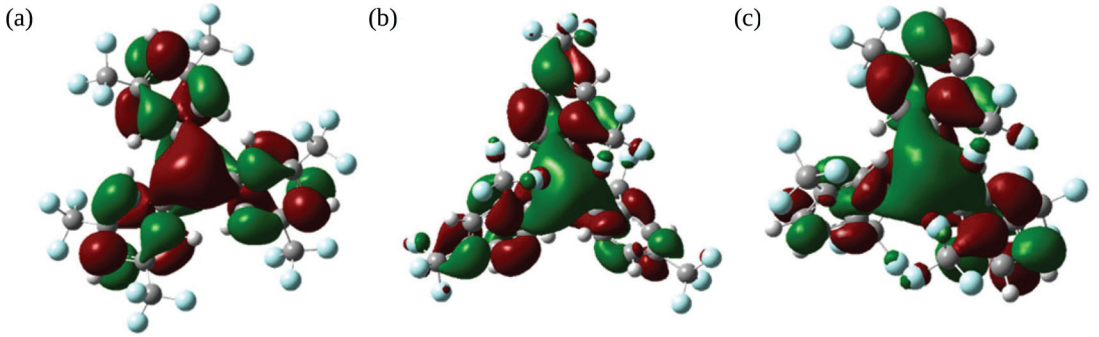

Fig. 7 Lowest unoccupied molecular orbitals (LUMOs) for (a) **1**, (b) **2**, and (c) **3**.

whilst the bridging-hydride species, $[(\mu\text{-H})(\mathbf{1})_2]^-$, is oxidized at an even more positive potential approaching that of the direct oxidation of H_2 at a GCE (*ca.* +1.5 V *vs.* $[FeCp_2]^{0/+}$), and is effectively behaving as an electrolyte under these conditions.

Computational studies

To further our understanding of the tris{bis(trifluoromethyl)-phenyl}borane isomers **1–3** we have investigated them and their associated radical-anions $\mathbf{1}^{\bullet-}$–$\mathbf{3}^{\bullet-}$ using density functional theory (DFT).

For all the neutral boranes **1–3** the LUMOs (Fig. 7) showed a high degree of boron p_z character (19, 22, 19% respectively, the majority of the remaining contributions being from the phenyl π-systems) as do the SOMOs (Fig. S4†) for the radical-anions $\mathbf{1}^{\bullet-}$–$\mathbf{3}^{\bullet-}$.

Total molecular energy calculations indicate that the ground state of **1** is lower in energy than those of **2** and **3** by *ca.* 43 kJ mol^{-1}. Analysis of calculated Mulliken atomic charges for **1–3**, show that any stabilisation of **1** compared to **2** and **3** cannot be attributed to electron withdrawing effects of the aryl rings; and therefore may be attributed to the reduced steric hindrance caused by the lack of *ortho*-CF_3 groups in **1**.

As noted previously, the *ortho*-CF_3 groups in **2** and **3** are orientated such that there is potential for B···F bonding interactions. Such interactions are clearly identified by the calculated bonding parameters: the B···F bonding parameter for **2** is 0.065, whilst for **3** it is 0.076 (in both cases averaged over all contributing B···F pairs). As expected, in **1**, where no interaction occurs, the B···F bonding parameter to the *meta*-CF_3 groups is <0.001.

Conclusions

We have investigated three structural isomers of tris{bis(trifluoromethyl)phenyl}borane in terms of both their electrochemical redox chemistries and also as the Lewis acidic components of an FLP for the heterolytic cleavage of H_2.

The two isomers of tris{bis(trifluoromethyl)phenyl}borane that incorporate *ortho*-CF_3 groups were not found to be active as the Lewis acidic component of FLPs for H_2 cleavage reactions. This lack of reactivity is due to a combination of, kinetic effects resulting from in part steric shielding of the boron centre; but also quenching of the boranes' electrophilicity through B···F bonding interactions, which are quantified by DFT calculations and electrochemical measurements. Whilst electrochemical studies show that all three isomers are less electrophilic than the archetypal Lewis acid $B(C_6F_5)_3$ the link between Lewis acidity, activity towards H_2 in an FLP, and electrophilicity, as shown in our previous studies[20,25,26] and those of other groups[33–35] is complex and requires further study.

The direct synthesis of all three tris{bis(trifluoromethyl)-phenyl}borohydride species under mild conditions allows for their reduction potentials to be measured, and their propensity for combined electrochemical-frustrated Lewis pair catalysis to be screened in a straightforward manner. The oxidation potentials of all three terminal borohydrides studied were found to be more positive than that of $[HB(C_6F_5)_3]^-$ yet are still less than the potential required for the direct oxidation of H_2 at a GCE under identical conditions.

Electrochemical studies of the bridging hydride formed when H_2 is cleaved by the $B\{3,5\text{-}(CF_3)_2C_6H_3\}_3$/tmp FLP, show that this species is oxidized at comparable potentials to that of the direct oxidation of H_2. However, following oxidation, the regeneration of the parent borane species is clearly observed, which is not the case for any of the terminal borohydride Na[**1**-H]–Na[**3**-H] species studied.

What this report demonstrates is the utility of electrochemical characterization methods to enable synthetic chemists to rapidly screen prospective new Lewis acids using simple electrochemical techniques to gain insights into the chemical behaviour of new species. It also provides insights to guide the design of new Lewis acids for researchers wishing to employ the combined electrochemical-frustrated Lewis pair activation of H_2, which is the focus of our ongoing studies.

Experimental

All reactions and manipulations were performed under an atmosphere of dry, oxygen-free N_2, using either standard Schlenk techniques or in either a MBraun UNIlab or LABmaster

glovebox. All solvents were dried prior to use by refluxing over an appropriate drying agent {Na/benzophenone for petroleum ether (b.p 40–60 °C) and diethyl ether; Na for toluene; CaH_2 for dichloromethane}, collected by distillation under an inert N_2 atmosphere and stored over 4 Å molecular sieves prior to use. All other reagents were obtained from commercial suppliers and used as received.

NMR Spectra were obtained on either a Bruker Avance III 500 MHz or Bruker AV 400 MHz spectrometer, all deuterated solvents were dried over 4 Å molecular sieves prior to use. For ^{1}H spectra residual *protio*-solvent was used as an internal standard; for ^{13}C the solvent resonance(s) were used as an internal standard;[36] for ^{19}F spectra $CFCl_3$ was used as an external standard; for ^{11}B spectra $BF_3{\cdot}Et_2O$ was used as an external standard. ^{1}H and ^{19}F DOSY experiments were performed on a Bruker Avance III 500 MHz spectrometer equipped with a broadband multinuclear probe, using a longitudinal eddy current delay incorporating bipolar gradients for diffusion and spoil gradients (ledbpgp2s) pulse sequence.[37]

Mass spectrometry was performed by the EPSRC Mass Spectrometry Service at the University of Swansea for **3**, or by Dr L. Haigh at Imperial College using a Micromass Autospec Premier spectrometer for **2**. Elemental analyses were performed by Mr S. Boyer of the Elemental Analysis Service at London Metropolitan University.

Single crystals of **3** were grown by slow diffusion of a saturated CH_2Cl_2 solution of the compound into *n*-hexane; data collection and processing was performed at the UK National Crystallographic Service at the University of Southampton.[30] Using Olex2,[38] the structure was solved and space group assigned with SuperFlip/EDMA[39] using charge flipping, and then refined with the ShelXL version 2014/7[40] refinement program using least squares minimization.

CCDC 1061234 contains the supplementary crystallographic data for this paper.

Electrochemical studies were carried out using a Metrohm Autolab PGSTAT302N potentiostat linked to a computer running Metrohm Autolab NOVA version 1.11 software, in conjunction with a three electrode cell comprising: a glassy carbon disc working electrode (Bioanalytical Systems Inc., *ca.* 7.0 mm^2 area calibrated using the $[FeCp_2]^{0/+}$ redox couple), a platinum wire (99.99% purity) counter electrode, and a silver wire (99.99% purity) *pseudo*-reference electrode; all electrodes were polished with 0.3 μm α-alumina and dried prior to use. All electrochemical measurements were performed at ambient temperature under a dry N_2 atmosphere, in CH_2Cl_2 containing 0.05 M $[^nBu_4N][B(C_6F_5)_4]$ as the supporting electrolyte and between 1.0 and 2.0 mM of the analyte species of interest. Cyclic voltammetric measurements were *i*R-compensated using positive-feedback to within 85 ± 5% of the uncompensated solution resistance. $[^nBu_4N][B(C_6F_5)_4]$ was synthesized according to published methods.[41] All potentials were referenced to the $[FeCp_2]^{0/+}$ redox couple, which was added as an internal standard. Simulations of electrochemical processes were performed using ElchSoft DigiElch version 7.096 software.[42]

DFT calculations were performed using the Gaussian 09 computational package.[43] Geometry optimization calculations have been carried out using the three-parameter exchange functional of Becke[44] (B3) and the correlation functional of Lee, Yang, and Parr (LYP), B3LYP.[45] The 6-311+G(d,p) basis set has been implemented for all atoms.[46] Structures were geometry optimized in the gas phase with the default convergence criteria and confirmed as minima through frequency calculations. All optimized structures were confirmed as minima by frequency analysis with thermodynamic properties extracted for the gas phase at 298.15 K and 1 atm. Bonding parameters between B and F atoms were calculated as the absolute values of the associated non-diagonal elements of the condensed to atoms electron density matrix. Density matrixes were computed in a separate calculation taking into consideration basis set superposition error (BSSE) correction using an unrestricted Hartree–Fock (H–F) calculation with counterpoise (CP) correction approach as implemented in Gaussian suite.

$B\{3,5\text{-}(CF_3)_2C_6H_3\}_3$ **1**[18,27] and $[tmpH][(\mu\text{-}H)(B\{3,5\text{-}(CF_3)_2C_6H_3\}_3)_2]$ $[tmpH][(\mu\text{-}H)(\mathbf{1})_2]$[18] were synthesized as previously reported.

$B\{2,4\text{-}(CF_3)_2C_6H_3\}_3$ 2

2,4-Bis(trifluoromethyl)bromobenzene (2.00 g, 1.16 cm^3, 6.83 mmol) and Et_2O (100 cm^3) were combined and the solution cooled to −77 °C. With the aid of rapid stirring, ^{n}BuLi (2.87 cm^3, 7.17 mmol, 2.5 M in hexanes) was added slowly by means of a syringe. Following one hour of stirring, BCl_3 (2.28 cm^3, 2.28 mmol, 1.0 M in heptane) was syringed into the amber solution and the mixture permitted to warm slowly to room temperature. The volatiles were removed *in vacuo* and the off white residue extracted with CH_2Cl_2 (3 × 25 cm^3) and filtered through Celite. Volatiles were removed under vacuum, and following a high vacuum sublimation step (10^{-6} mbar) at 85 °C, a pure white solid was obtained. Yield 1.33 g (2.04 mmol, 90%).

^{1}H NMR (400.4 MHz, CD_2Cl_2, 25 °C, δ): +8.06 (s, 3H, 3-H), +7.87 (d, 3H, $^3J_{HH}$ = 8 Hz, 5-H), +7.46 (d, 3H, $^3J_{HH}$ = 8 Hz, 6-H); ^{11}B NMR (128.4 MHz, CD_2Cl_2, 25 °C, δ): +74.0 (br.s); ^{13}C{^{1}H} NMR (100.6 MHz, CD_2Cl_2, 25 °C, δ): +144.2 (br, 1-C), +135.9 (s, 6-CH), +134.2 (q, $^2J_{CF}$ = 34 Hz, 2/4-C), +133.7 (q, $^2J_{CF}$ = 34 Hz, 2/4-C), +127.9 (q, $^3J_{CF}$ = 3 Hz, 5-CH), +123.9 (q, $^1J_{CF}$ = 273 Hz, 2/4-CF_3), +123.6 (sept., $^3J_{CF}$ = 3 Hz, 3-CH), +123.6 (q, $^1J_{CF}$ = 273 Hz, 2/4-CF_3). ^{19}F NMR (376.8 MHz, CD_2Cl_2, 25 °C, δ): −56.6 (s, 9F, 2-CF_3), −63.8 s, 9F, 4-CF_3). HRMS-EI (*m*/*z*): $[M]^+$ calc. for $C_{24}H_9BF_{18}$, 650.0510; found, 650.0491. Elemental analysis (calc. for $C_{24}H_9B_1F_{18}$): C 44.34 (44.48), H 1.40 (1.47).

$B\{2,5\text{-}(CF_3)_2C_6H_3\}_3$ 3

2,5-Bis(trifluoromethyl)bromobenzene (3.1 cm^3, 17.9 mmol) and Et_2O (100 cm^3) were combined and cooled to −77 °C. ^{n}BuLi (11 cm^3, 17.6 mmol, 1.6 M in hexanes) was added to the stirred solution. After one hour BCl_3 (5.8 cm^3, 5.8 mmol, 1.0 M in heptane) was added to the orange solution and the mixture permitted to slowly warm to room temperature. The volatiles were removed *in vacuo* and the pale yellow residue extracted

with CH_2Cl_2 (3 × 25 cm^3) and filtered (*via* cannula). The product is then recrystallized from CH_2Cl_2/*n*-hexane and isolated as a white micro-crystalline solid. Yield 2.89 g (4.44 mmol, 77%).

^{1}H NMR (500.21 MHz, CD_2Cl_2, 25 °C, δ): +7.95 (s, 3H, 3/4-H), +7.95 (s, 3H, 3/4-H), +7.47 (s, 3H, 6-H); ^{11}B NMR (160.49 MHz, CD_2Cl_2, 25 °C, δ): +70.7 (br.s); ^{13}C{^{1}H} NMR (125.78 MHz, CD_2Cl_2, 25 °C, δ): +141.5 (br.s, 1-C), +137.1 (q, $^2J_{CF}$ = 33 Hz, 2/5-C), +133.3 (q, $^2J_{CF}$ = 33 Hz, 2/5-C), +132.4 (q, $^3J_{CF}$ = 3.7 Hz, 3/4/6-C), +129.3 (q, $^3J_{CF}$ = 3.7 Hz, 3/4/6-C), +127.8 (br.m, 3/4/6-C), +124.1 (q, $^1J_{CF}$ = 275 Hz, 2/5-CF_3), +123.9 (q, $^1J_{CF}$ 273 Hz, 2/5-CF_3); ^{19}F NMR (470.67 MHz, CD_2Cl_2, 25 °C, δ): −56.5 (s, 9F, 2-CF_3), −63.7 (s, 9F, 5-CF_3). HRMS-APCI (*m*/*z*): $[M - F]^+$ calc. for $C_{24}H_9BF_{17}$, 631.0525; found, 631.0519. Elemental analysis (calc. for $C_{24}H_9B_1F_{18}$): C 44.22 (44.48), H 1.38 (1.47).

Na[HB{3,5-$(CF_3)_2C_6H_3$}$_3$] Na[1-H]

To a solution of **1** (0.40 g, 0.62 mmol) in toluene (10 cm^3) was added Na[$HBEt_3$] (0.6 cm^3, 0.6 mmol, 1.0 M in toluene), the reaction mixture was stirred for 6 hours to give a colourless solution. All volatiles were removed *in vacuo*, to give a white residue which was washed with petroleum ether (2 × 5 cm^3) and dried *in vacuo* to give a white solid. Yield 0.40 g (0.59 mmol, 95%).

^{1}H NMR (500.21 MHz, CD_3CN, 25 °C, δ): +7.70 (s, 6H, 2,6-H), +7.58 (s, 3H, 4-H), +3.66 (br.q, $^1J_{HB}$ = 84 Hz, 1H, HB); ^{11}B NMR (160.49 MHz, CD_3CN, 25 °C, δ): −9.1 (d, $^1J_{BH}$ = 88 Hz); ^{13}C{^{1}H} NMR (125.78 MHz, CD_3CN, 25 °C, δ): +165.0 (q, $^1J_{CF}$ = 49 Hz, 1-C), +135.7 (s, 2,6-C), +130.1 (q, $^2J_{CF}$ = 32 Hz, 3,5-C), +126.0 (q, $^1J_{CF}$ = 272 Hz, CF_3), +118.5 (s, 4-C); ^{19}F NMR (470.67 MHz, CD_3CN, 25 °C, δ): −63.0 (s, 18F, CF_3). Elemental analysis (calc. for $C_{24}H_{10}B_1F_{18}Na$): C 42.95 (42.76), H 1.61 (1.50).

Na[HB{2,4-$(CF_3)_2C_6H_3$}$_3$] Na[2-H]

To a solution of **2** (0.275 g, 0.42 mmol) in toluene (8 cm^3) was added Na[$HBEt_3$] (0.43 cm^3, 0.43 mmol, 1.0 M in toluene), the reaction mixture was stirred for 4 hours to give a cloudy white suspension. The reaction mixture was concentrated *in vacuo* reducing its volume to *ca*. 2 cm^3, and the product precipitated by addition of petroleum ether and cooling to −25 °C. The white solid was isolated by filtration and dried *in vacuo*. Yield 0.231 g (0.34 mmol, 81%).

^{1}H NMR (500.21 MHz, CD_3CN, 25 °C, δ): +7.76 (s, 3H, 3-H), +7.47 (d, $^3J_{HH}$ = 7.9 Hz, 3H, 5-H), +7.11 (d, $^3J_{HH}$ = 7.9 Hz, 3H, 6-H), +4.06 (br.q, $^1J_{HB}$ = 93 Hz, 1H, BH); ^{11}B NMR (160.49 MHz, CD_3CN, 25 °C, δ): −15.33 (d, $^1J_{BH}$ = 93 Hz); ^{13}C{^{1}H} NMR (125.78 MHz, CD_3CN, 25 °C, δ): +139.1 (s, 6-CH), +135.3 (q, $^2J_{CF}$ = 29 Hz, 2/4-C), +126.7 (q, $^3J_{CF}$ = 3.7 Hz, 5-CH), +126.7 (q, $^1J_{CF}$ = 275 Hz, 2/4-CF_3), +126.3 (q, $^2J_{CF}$ = 32 Hz, 2/4-C), +126.2 (q, $^1J_{CF}$ = 272 Hz, 2/4-CF_3), +122.6 (sept., $^3J_{CF}$ = 3.7 Hz, 3-CH),; ^{19}F NMR (470.67 MHz, CD_3CN, 25 °C, δ): −59.5 (d, J_{FH} = 6.8 Hz, 9F, 2-CF_3), −62.6 (s, 9F, 4-CF_3). Elemental analysis (calc. for $C_{24}H_{10}B_1F_{18}Na$): C 42.83 (42.76), H 1.57 (1.50).

Na[HB{2,5-$(CF_3)_2C_6H_3$}$_3$] Na[3-H]

To a solution of **3** (0.275 g, 0.42 mmol) in toluene (8 cm^3) was added Na[$HBEt_3$] (0.43 cm^3, 0.43 mmol, 1.0 M in toluene), the reaction mixture was stirred for 4 hours to give a colourless solution. The reaction mixture was concentrated *in vacuo* reducing its volume to *ca*. 2 cm^3, and the product crystallized by addition of petroleum ether and cooling to −25 °C. The white crystalline solid was isolated by filtration and dried *in vacuo*. Yield 0.207 g (0.31 mmol, 74%).

^{1}H NMR (500.21 MHz, CD_2Cl_2, 25 °C, δ): +7.70 (d, $^3J_{HH}$ = 8.2 Hz, 3H, 3/4-H), +7.45 (d, $^3J_{HH}$ = 8.5 Hz, 3H, 3/4-H), +7.23 (br.s, 3H, 6-H), +3.06 (br.qq, $^1J_{HB}$ = 82 Hz, $J_{HF} \approx$ 9.1 Hz, 1H, BH); ^{11}B NMR (160.49 MHz, CD_2Cl_2, 25 °C, δ): −14.23 (d, $^1J_{BH}$ = 84 Hz); ^{13}C{^{1}H} NMR (125.78 MHz, CD_2Cl_2, 25 °C, δ): +134.8 (q, $^2J_{CF}$ = 28.0 Hz, 2/5-C), +133.7 (q, $^3J_{CF}$ = 3.7 Hz, 3/4/6-C), +132.3 (q, $^2J_{CF}$ = 31.0 Hz, 2/5-C), +127.1 (q, $^1J_{CF}$ = 275 Hz, 2/5-CF_3), +126.3 (br.m, 3/4/6-C), +124.9 (q, $^1J_{CF}$ = 273 Hz, 2/5-CF_3), +121.6 (q, $^3J_{CF}$ 3.9 Hz, 3/4/6-C); ^{19}F NMR (470.67 MHz, CD_2Cl_2, 25 °C, δ): −59.3 (d, J_{FH} = 7.6 Hz, 9F, 2-CF_3), −63.6 (s, 9F, 5-CF_3). Elemental analysis (calc. for $C_{24}H_{10}B_1F_{18}Na$): C 42.93 (42.76), H 1.61 (1.50).

Acknowledgements

G. G. W. and A. E. A. thank the Royal Society for financial support by University Research Fellowships. E. J. L. thanks the EPSRC for financial support by a DTA studentship under grant number EP/J500409. The research leading to these results has received funding from the European Research Council under the ERC Grant Agreement no. 307061 (PiHOMER).

We thank Dr C. MacDonald (University of East Anglia) for assistance with the ^{1}H and ^{19}F DOSY NMR experiments.

We acknowledge the use of the EPSRC funded National Chemical Database Service hosted by the Royal Society of Chemistry, and the EPSRC UK National Mass Spectrometry Facility (NMSF) at the University of Swansea. We thank the EPSRC UK National Crystallography Service at the University of Southampton for the collection of the crystallographic data.[30] We thank the Research Computing Service at the University of East Anglia for access to the high performance computing cluster.

References

1 G. C. Welch and D. W. Stephan, *J. Am. Chem. Soc.*, 2007, **129**, 1880–1881.
2 D. W. Stephan, *Dalton Trans.*, 2009, 3129–3136.
3 D. W. Stephan and G. Erker, *Angew. Chem., Int. Ed.*, 2010, **49**, 46–76.
4 D. W. Stephan, *Comp. Inorg. Chem. II*, 2013, **1**, 1069–1103.
5 D. W. Stephan and G. Erker, *Chem. Sci.*, 2014, **5**, 2625–2641.
6 D. W. Stephan, *Acc. Chem. Res.*, 2015, **48**, 306–316.

7 D. W. Stephan and G. Erker, *Angew. Chem., Int. Ed.*, 2015, **54**, 6400–6441.
8 P. A. Chase, G. C. Welch, T. Jurca and D. W. Stephan, *Angew. Chem., Int. Ed.*, 2007, **46**, 8050–8053.
9 K. Chernichenko, Á. Madarász, I. Pápai, M. Nieger, M. Leskelä and T. Repo, *Nat. Chem.*, 2013, **5**, 718–723.
10 H. Wang, R. Fröhlich, G. Kehra and G. Erker, *Chem. Commun.*, 2008, 5966–5968.
11 T. Mahdi and D. W. Stephan, *J. Am. Chem. Soc.*, 2012, **136**, 15809–15812.
12 D. J. Scott, M. J. Fuchter and A. E. Ashley, *J. Am. Chem. Soc.*, 2014, **136**, 15813–15816.
13 G. Ménard, T. M. Gilbert, J. A. Hatnean, A. Kraft, I. Krossing and D. W. Stephan, *Organometallics*, 2013, **32**, 4416–4422.
14 Z. Lu, Y. Wang, J. Liu, Y. Lin, Z. H. Li and H. Wang, *Organometallics*, 2013, **32**, 6753–6758.
15 R. L. Melen, *Chem. Commun.*, 2014, **50**, 1161–1174.
16 S. C. Binding, H. Zaher, F. M. Chadwicka and D. O'Hare, *Dalton Trans.*, 2012, **41**, 9061–9066.
17 D. J. Scott, M. J. Fuchter and A. E. Ashley, *Angew. Chem., Int. Ed.*, 2014, **53**, 10218–10222.
18 T. J. Herrington, A. J. W. Thom, A. J. P. White and A. E. Ashley, *Dalton Trans.*, 2012, **41**, 9019–9022.
19 J. M. Farrell, J. A. Hatnean and D. W. Stephan, *J. Am. Chem. Soc.*, 2012, **134**, 15728–15731.
20 E. J. Lawrence, T. J. Herrington, A. E. Ashley and G. G. Wildgoose, *Angew. Chem., Int. Ed.*, 2014, **53**, 9922–9925.
21 G. Ménard and D. W. Stephan, *Angew. Chem., Int. Ed.*, 2012, **53**, 8272–8275.
22 E. R. Clark and M. J. Ingleson, *Angew. Chem., Int. Ed.*, 2014, **53**, 11306–11309.
23 A. M. Chapman, M. F. Haddow and D. F. Wass, *J. Am. Chem. Soc.*, 2011, **133**, 18463–18478.
24 X. Xu, G. Kehr, C. G. Daniliuc and G. Erker, *J. Am. Chem. Soc.*, 2015, **137**, 4550–4557.
25 E. J. Lawrence, V. S. Oganesyan, D. L. Hughes, A. E. Ashley and G. G. Wildgoose, *J. Am. Chem. Soc.*, 2014, **136**, 6031–6036.
26 E. J. Lawrence, R. J. Blagg, D. L. Hughes, A. E. Ashley and G. G. Wildgoose, *Chem. – Eur. J.*, 2015, **21**, 900–906.
27 E. L. Kolychev, T. Bannenberg, M. Freytag, C. G. Daniliuc, P. G. Jones and P. D. M. Tamm, *Chem. – Eur. J.*, 2012, **18**, 16938–16946.
28 S. M. Cornet, K. B. Dillon, C. D. Entwistle, M. A. Fox, A. E. Goeta, H. P. Goodwin, T. B. Marder and A. L. Thompson, *Dalton Trans.*, 2003, 4395–4405.
29 W. V. Konze, B. L. Scott and G. J. Kubas, *Chem. Commun.*, 1999, 1807–1808.
30 S. J. Coles and P. A. Gale, *Chem. Sci.*, 2012, **3**, 683–689.
31 E. J. Lawrence, V. S. Oganesyan, G. G. Wildgoose and A. E. Ashley, *Dalton Trans.*, 2013, **42**, 782–789.
32 D. H. McDaniel and H. C. Brown, *J. Org. Chem.*, 1958, **23**, 420–427.
33 T. A. Rokob, A. Hamza and I. Pápai, *J. Am. Chem. Soc.*, 2009, **131**, 10701–10710.
34 I. B. Sivaev and V. I. Bregadze, *Coord. Chem. Rev.*, 2014, **270–271**, 75–88.
35 Z. M. Heiden and A. P. Lathem, *Organometallics*, 2015, **34**, 1818–1827.
36 G. R. Fulmer, A. J. M. Miller, N. H. Sherden, H. E. Gottlieb, A. Nudelman, B. M. Stoltz, J. E. Bercaw and K. I. Goldberg, *Organometallics*, 2010, **29**, 2176–2179.
37 D. H. Wu, A. D. Chen and C. S. Johnson, *J. Magn. Reson., Ser. A*, 1995, **115**, 260–264.
38 L. J. Bourhis, O. V. Dolomanov, R. J. Gildea, J. A. K. Howard and H. Puschmann, *Acta Crystallogr., Sect. A: Fundam. Crystallogr.*, 2015, **71**, 59–75; O. V. Dolomanov, L. J. Bourhis, R. J. Gildea, J. A. K. Howard and H. Puschmann, *J. Appl. Crystallogr.*, 2009, **42**, 339–341.
39 L. Palatinus and G. Chapuis, *J. Appl. Crystallogr.*, 2007, **40**, 786–790; L. Palatinus and A. van der Lee, *J. Appl. Crystallogr.*, 2008, **41**, 975–984; L. Palatinus, S. J. Prathapab and S. van Smaalen, *J. Appl. Crystallogr.*, 2012, **45**, 575–580.
40 G. M. Sheldrick, *Acta Crystallogr., Sect. C: Cryst. Struct. Commun.*, 2015, **71**, 3–8; G. M. Sheldrick, *Acta Crystallogr., Sect. A: Fundam. Crystallogr.*, 2008, **64**, 112–122.
41 S. Lancaster, *ChemSpider Synthetic Pages*, 2003, DOI: 10.1039/SP215, http://cssp.chemspider.com/215; T. E. Krattf, Boulder Scientific Company, *Eur. Pat*, 1186608, 2002; R. J. LeSuer, C. Buttolph and W. E. Geiger, *Anal. Chem.*, 2004, **76**, 6395–6401.
42 *DigiElch-Professional*, ElechSoft, Kleinromstedt, Germany.
43 M. J. Frisch, G. W. Trucks, H. B. Schlegel, G. E. Scuseria, M. A. Robb, J. R. Cheeseman, G. Scalmani, V. Barone, B. Mennucci, G. A. Petersson, H. Nakatsuji, M. Caricato, X. Li, H. P. Hratchian, A. F. Izmaylov, J. Bloino, G. Zheng, J. L. Sonnenberg, M. Hada, M. Ehara, K. Toyota, R. Fukuda, J. Hasegawa, M. Ishida, T. Nakajima, Y. Honda, O. Kitao, H. Nakai, T. Vreven, J. A. Montgomery, J. E. Peralta Jr., F. Ogliaro, M. Bearpark, J. J. Heyd, E. Brothers, K. N. Kudin, V. N. Staroverov, R. Kobayashi, J. Normand, K. Raghavachari, A. Rendell, J. C. Burant, S. S. Iyengar, J. Tomasi, M. Cossi, N. Rega, J. M. Millam, M. Klene, J. E. Knox, J. B. Cross, V. Bakken, C. Adamo, J. Jaramillo, R. Gomperts, R. E. Stratmann, O. Yazyev, A. J. Austin, R. Cammi, C. Pomelli, J. W. Ochterski, R. L. Martin, K. Morokuma, V. G. Zakrzewski, G. A. Voth, P. Salvador, J. J. Dannenberg, S. Dapprich, A. D. Daniels, O. Farkas, J. B. Foresman, J. V. Ortiz, J. Cioslowski and D. J. Fox, *Gaussian 09, revision A.02*, Gaussian, Inc., Wallingford, CT, 2009.
44 A. D. Becke, *J. Chem. Phys.*, 1993, **98**, 5648–5652.
45 C. Lee, W. Yang and R. G. Parr, *Phys. Rev. B: Condens. Matter*, 1988, **37**, 785–789.
46 P. C. Hariharan and J. A. Pople, *Theor. Chim. Acta*, 1973, **28**, 213–222.